Journal of Applied Polymer Science

Thermal Stability and Ablation Properties Study of Aluminum Silicate Ceramic Fiber and Acicular Wollastonite Filled Silicone Rubber Composite

Lin Yu, Shengtai Zhou, Huawei Zou, Mei Liang
The State Key Lab of Polymer Materials Engineering, Polymer Research Institute of Sichuan University, Chengdu 610065, China
Correspondence to: H. Zou (E-mail: hwzou@163.com)

ABSTRACT: The thermal stability and ablation properties of silicone rubber filled with silica (SiO_2), aluminum silicate ceramic fiber (ASF), and acicular wollastonite (AW) were studied in this article. The morphology, composition, and ablation properties of the composite were analyzed after oxyacetylene torch tests. There were three different ceramic layers found in the ablated composite. In the porous ceramic layer, the rubber was decomposed, producing trimers, tetramers, and SiO_2. ASF and part of AW still remained and formed a dense layer. The SiO_2/SiC filaments in the ceramic layer reduced the permeability of oxygen, improving the ablation properties of the composites. The resultant ceramic layer was the densest, which acted as effective oxygen and heat barriers, and the achieved line ablation rate of the silicone composite were optimum at the proportion of 20 phr/40 phr (ASF/AW). Thermogravimetric analysis (TGA) confirmed that thermal stability of the composites was enhanced by the incorporation of ASF and AW. The formation of the ceramic layer was considered to be responsible for the enhancement of thermal stability and ablation properties. © 2013 Wiley Periodicals, Inc. J. Appl. Polym. Sci. **2014**, *131*, 39700.

KEYWORDS: composites; rubber; thermal properties; thermogravimetric analysis (TGA)

Received 9 May 2013; accepted 23 June 2013
DOI: 10.1002/app.39700

INTRODUCTION

Recently, polymeric composites were widely investigated in aerospace industry for severe condition applications.[1–6] Polydimethylsiloxane (PDMS) is widely used as antiablation polymer for containing —Si—O— bonds in the backbone, which has attracted considerable attention due to its excellent thermal stability at 400°C and high residual yield (53% at 1100°C) in nitrogen atmosphere.[7] However, PDMS can be burnt away and only form a very weak powdered char on the surface at severely high temperatures, displaying weak ablation properties.[8]

To improve the residual yield, a wide range of reinforcements are applied to the polymeric matrix. Kim et al.[8] incorporated carbon fiber (CF) and silicon carbide (SiC) into PDMS, and enhanced hardness of the composite char surface was obtained, which was an important factor determining the ablation properties. However, the addition of CF into the composites reduced the thermal stability, for the high thermal conductivity of CF.[9–11] In addition, aluminum silicate ceramic fiber (ASF) demonstrated low thermal conductivity (0.128 W m^{-1} K^{-1}), which was beneficial to thermal stability of composites and found application as a refractory.[12] Silicone rubber filled with silicate (muscovite mica) formed a coherent and strong residual after exposure to elevated temperatures.[13,14] Inorganic compounds such as zirconium carbide (ZrC), zirconia (ZrO_2), silicon carbide (SiC) can greatly improve the thermal and ablation properties.[6,8] However, carbonaceous filler, like CF and metallic filler exhibit high thermal conductivity, which is unfavorable for thermal stability of the composites. The acicular wollastonite (AW) with a certain length–diameter ratio and low thermal conductivity improves the thermal stability and makes the ceramic layer denser. There are a large number of the hydroxyl groups on the surface of AW,[15] so it is easy to combine with silicone rubber like SiO_2 integrated with PDMS. While compared with PDMS, polymethylvinylsiloxane (PMVS) is easier to vulcanize which is mainly due to its content of vinyl side chains. Although a variety of fillers have been investigated as candidate for ablation studies, the low thermal conductivity filler with a certain length-diameter ratio has seldom been discussed.

In this article, ASF (0.128 W m^{-1} K^{-1}) and AW (2.5 W m^{-1} K^{-1}) were used as fillers for their low thermal conductivity, which was expected to make a low thermally conducting shield and hinder the heat flux from penetrating into the internal matrix under oxyacetylene fire. The experimental idea has few reported. The refractory materials (ASF and AW) with a certain length–diameter ratio were expected to make the ceramic layer denser

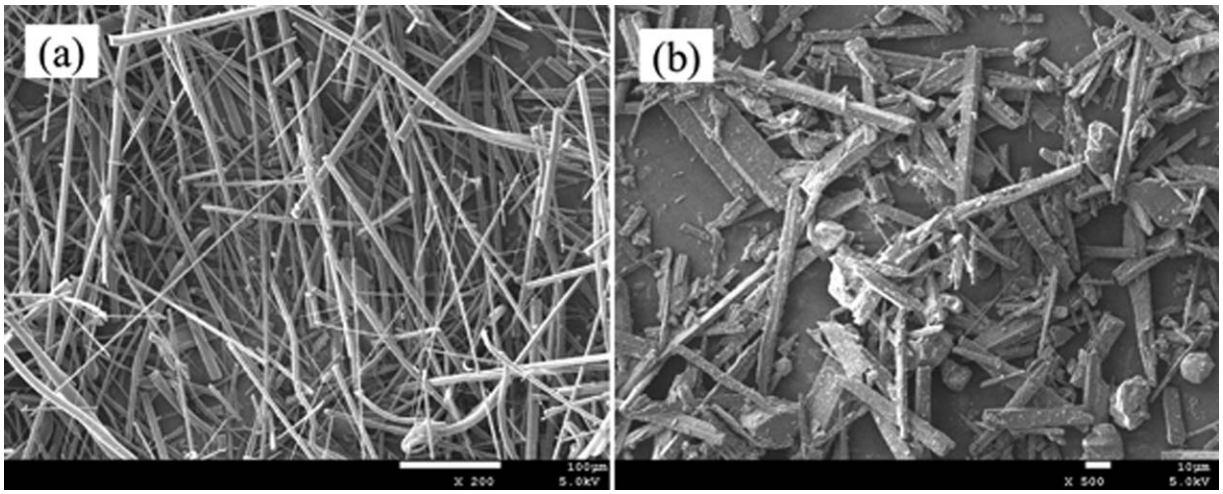

Figure 1. SEM image of the (a) ASF and (b) AW.

and effectively provide barriers for oxygen diffusion. The effect of ASF and AW on morphology, thermal stability, ablation properties and the components of ceramic layer of silicone-based composites were analyzed in this research.

EXPERIMENTAL

Materials

Commercial polymethylvinylsiloxane (PMVS) was purchased from Wynca Chemical, China. The average molecular weight was about 640,000 g mole^{-1}. The vinyl content of the rubber was 0.16% per mole. Fumed silica (SiO_2, Degussa, Germany) was used to enhance the breaking strength and tenacity of the composites. Dicumyl peroxide (DCP) was used as a curing agent, which was supplied by Chengdu Kelong Chemical Reagents Factory, China. AW was obtained from Jiangxi Huanyu, China. In cooperation with AW, ASF (Nanjing Suowo Technology, China) was used as fire resistance ingredient. The morphology of ASF and AW were clearly shown in Figure 1. ASF exhibits typical fiber morphology, whereas AW shows an irregular geometry.

Sample Preparation

The composites were prepared using a two-roll mill at room temperature. Silicone rubber was added first and then relevant fillers were added in turn. The whole process lasted 5 min., after which the curing agent was added and then processed for another 5 min at about 40°C.

The refolded sheet were molded and cured into flat sheets by compression molding at 175°C for 15min under the pressure of 10 MPa. The secondary vulcanization process was carried out at 200°C in the airflow drier for 2 h.

Ablation Process

Ablation experiments were conducted using oxyacetylene torch. The samples were compression-molded with a dimension of 40 mm × 40 mm × 7.5 mm. The flow rate of oxygen (O_2) and acetylene (C_2H_2) were 0.30 and 0.24 m^3 h^{-1}, respectively. The specimen was placed vertically to the flame direction in air. The distance between the nozzle tip of the oxyacetylene gun and the front surface of the specimen was 10 mm and the inner diameter of the tip was 1.6 mm. The surface temperature of the samples was about 1800°C, which was monitored by an optical pyrometer. The ablation duration for each sample was deliberately fixed at 60 s. The line ablation rate (R_d) can be calculated with the following equation:

$$R_d = \frac{\Delta d}{t} = \frac{d_1 - d_2}{t}$$

where d_1 is the original thickness (mm) of the specimen before ablation treatment and d_2 (mm) is the resultant thickness after ablation treatment. t represents the ablation time (s) during the fire treatment process. The unit of R_d is mm s^{-1}.

CHARACTERIZATIONS

Morphologic Study

The morphology of the composite after ablation process was characterized by scanning electron microscopy (SEM, JSM-5900, JOEL, Japan). The elemental distribution of the ablative composite after ablation was studied using energy dispersive spectroscopy (EDS, X-Max 51-XMX0019, OIMS, Britain).

Thermogravimetric Analysis

Thermogravimetric measurements were conducted with the help of thermogravimetric analyzer (TG 209F1 Iris, NETZSCH, Germany) to investigate the thermal stability of the samples under dry nitrogen gas conditions. The samples weighed about 10 mg. Then a series of samples were heated at a rate of 10°C min^{-1} and the relative mass loss of the samples was recorded from 40 to 800°C.

X-ray Diffraction (XRD)

X-ray diffraction (XRD) scans of the composites after ablation treatment were carried out on a D/MAX-III X-ray diffractometer (DY1291, Philips, Holland) with Cu Kα radiation ($\lambda = 0.1542$ nm) at a generator voltage of 40 kV and a generator current of 35 mA. The scan was conducted from a 2θ angle of 2° to 60° with a step interval of 0.03°.

Fourier Transformation Infrared (FTIR) Measurements

Fourier transformation infrared (FTIR) spectra were obtained in the range of 4000–400 cm^{-1} with a resolution of 1 cm^{-1} using a Nicolet iZ10 FTIR spectrophotometer, employing the potassium bromide (KBr) pellet technique.[16]

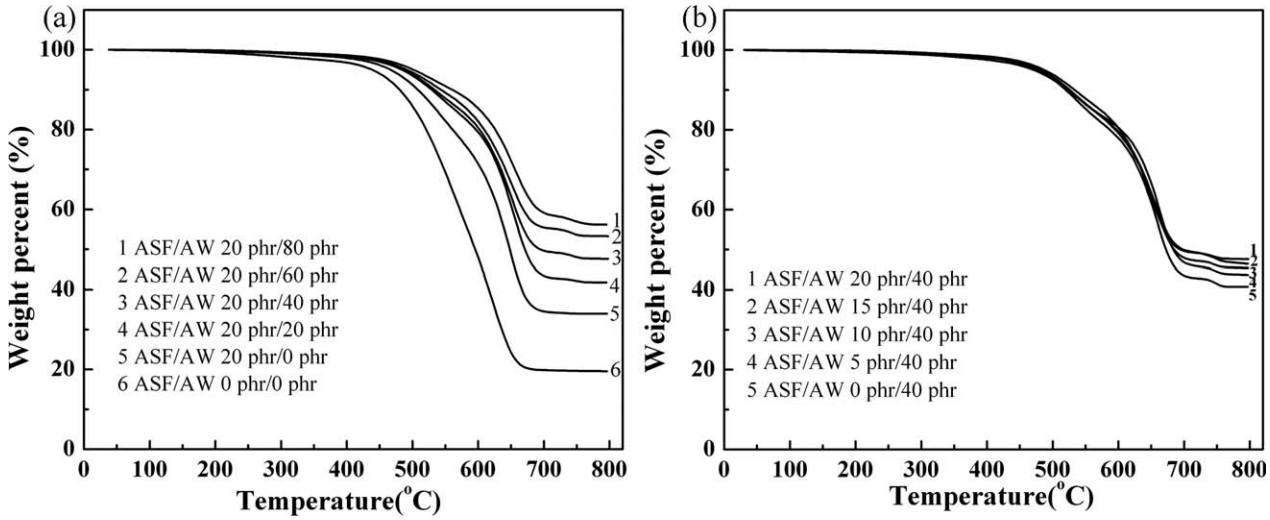

Figure 2. TGA curves for composites formed for (a) fixed ASF (20 phr) and (b) fixed AW (40 phr).

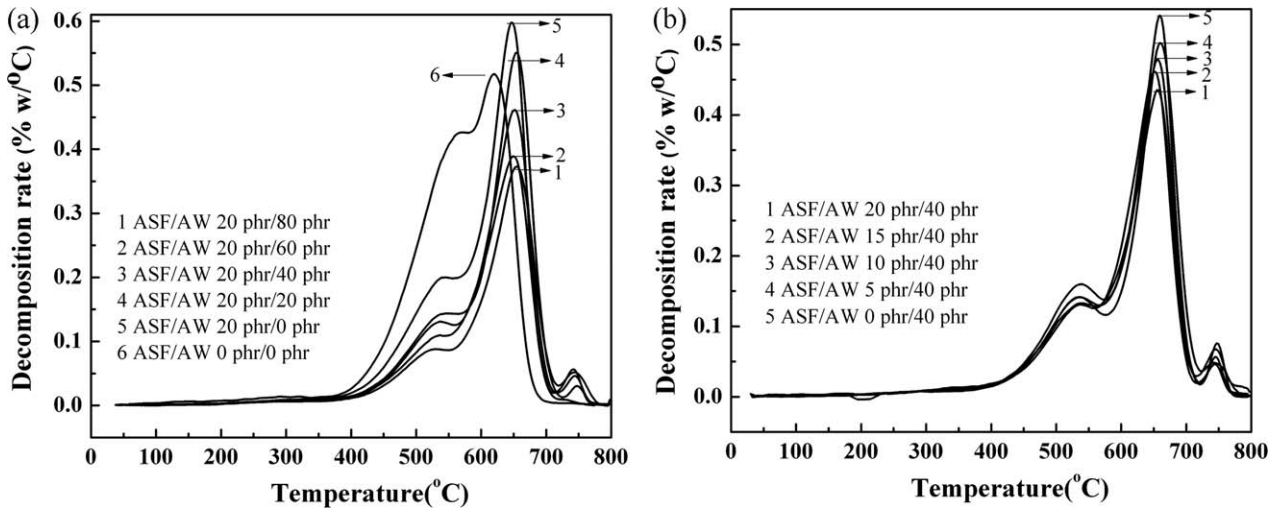

Figure 3. DTG curves for composites formed for (a) fixed ASF (20 phr) and (b) fixed AW (40 phr).

RESULTS AND DISCUSSION

Thermogravimetric Analysis (TGA)

The TGA and derivative thermograms (DTG) as a function of temperature for both ASF and AW filled silicone composites are presented in Figures 2 and 3, respectively. The characteristic data of TGA and DTG curves are listed in Table I.

The onset decomposition temperature (T_{onset}) is the temperature at 5% weight loss, and the residual yield at 800°C is defined as R_{800}. As shown in Table I, T_{onset} and R_{800} increased gradually with the increasing content of ASF and/or AW. It is shown in Figure 3(a) that the thermal degradation of silicon rubber composites takes a two mass loss steps. The first step was attributed to the thermal oxidation of the methyl branches during the temperature range from 400 to 570°C, producing methane and other organic gas. The other might be ascribed to the depolymerization of the siloxane chains during 570–720°C by producing cyclic trimers or tetramers.[17] Unlike the neat PMVS, the main decomposition reaction and weight loss of the composites mainly occurred in the second process. There was an ~75% of the

Table I. Thermal Degradation of Silicone-Based Polymer Composites in Nitrogen

ASF/AW	T_{onset} (°C)	Mass loss in the first step (%)	Mass loss n the second step (%)	R_{800} (%)
0/0	439	48.1	32.4	19.5
20/0	467	19.0	47.0	34.0
20/20	483	14.0	44.2	41.8
20/40	487	13.1	39.3	47.6
20/60	491	11.0	35.7	53.3
20/80	502	8.5	35.3	56.2
0/40	476	18.2	41.1	40.7
5/40	482	16.4	39.9	43.7
10/40	480	15.7	38.9	45.4
15/40	472	14.8	38.7	46.5
20/40	487	13.1	39.3	47.6

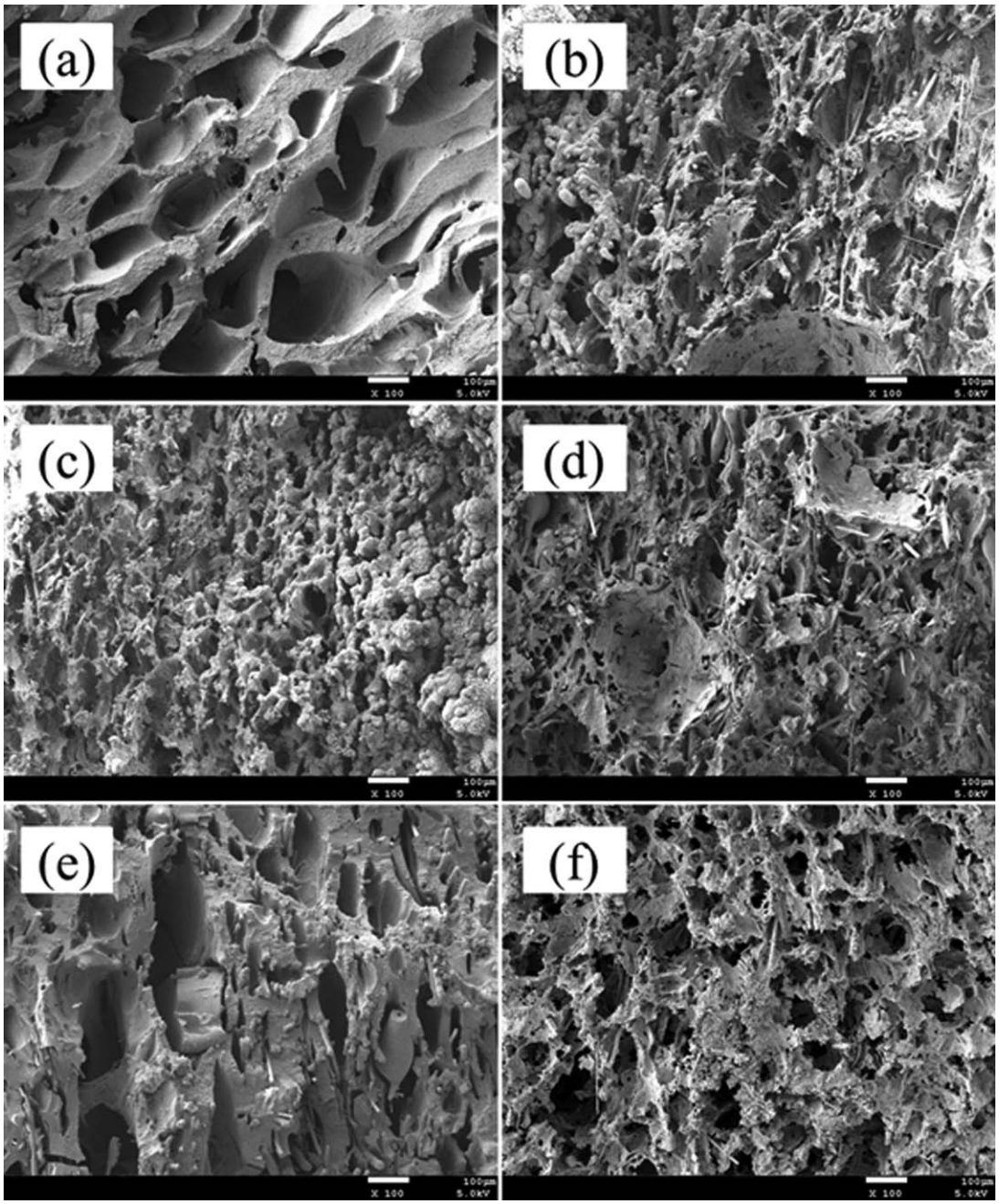

Figure 4. Transection morphology of the composites after ablation, the ratio of ASF /AW (a) 0 phr/0 phr, (b) 15 phr/40 phr, (c) 0 phr/40 phr, (d) 20 phr/40 phr, (e) 20 phr/0 phr, (f) 20 phr/80 phr.

weight loss happened in this degradation segment. TGA results revealed that thermal stability of the ASF and AW modified silicone rubber was improved effectively compared with that of the neat rubber, which was mainly attributed to the lower thermally conductive surface layer formed during the heat treatment process, hindering the heat flux from penetrating into the internal matrix. The reaction of AW on the composites was responsible for the slight weight loss observed from 720 to 780°C.

Morphology Study

The formation of the ceramic layer during oxyacetylene fire treatment process hinders the penetration of heat and oxygen from the sample surface, which decreases the decomposition of the internal matrix, and reduces the surface erosion rate of the composites. The rapid increase of temperature in the sample surface would generate strong heat stress, which arises from the escape of the pyrolysis gases and thermal expansion in the boundary of the ceramic layer. However, if the rubber matrix was not reinforced enough, the degraded material could easily break away, thus increasing the surface erosion rate.

As shown in Figure 4(a,c,e), the addition of ASF and AW enhanced the surface layer by forming a frame, making the porous ceramic layer denser. Figure 4(b–d) demonstrated that

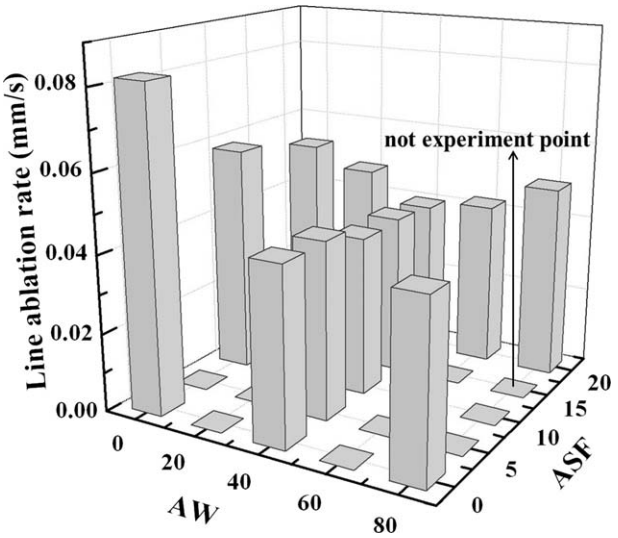

Figure 5. Line ablation rate of silicone rubber composites with different content of ASF and AW.

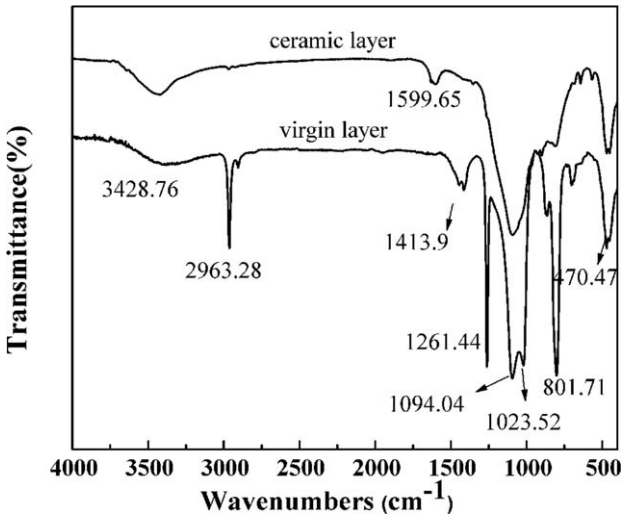

Figure 6. FTIR spectra for ceramic layer and virgin layer.

the pores of the frame changed smaller with the increase of ASF in the ablation samples. Moreover, Figure 4(d–f) showed that with the increase of AW in the composites also made the ceramic layer denser, which favored the antiablation ability of the composites. However, too much AW might induce the formation of bigger pores and weaker frame during the ablation process. The superior ceramic layer emerged with the proportion of ASF/AW in 20/40 phr. In addition, the low thermal conductivity of ASF and AW also hindered the heat penetration and enhanced ablation properties.

Ablation Properties of the Composites

As shown in Figure 5 that with the increase of ASF (the AW content was 0 phr), the line ablation rate decreased significantly. However, the line ablation rate decreased slowly with the increase of ASF while AW content was fixed to 40 phr. On the other hand, when AW was fixed to 80 phr, the incorporation of 20 phr ASF caused much higher ablation rate compared with that without the ASF. Interestingly, the ablation rate experienced a concave trend with the increase of AW while the ASF was fixed to 20 phr, which was considered the synergistic effect of ASF and AW. The line ablation rate reached a minimum at the proportion of 20/40 phr (ASF/AW). On one hand, the low thermal conductivity of the filler kept the heat flux from penetrating into the internal. Besides, the dense ceramic layer was also an efficient shield from flame to enhance the ablation resistance.

Component of the Ceramic Layer

Figure 6 showed the FTIR spectra of the virgin layer and the subsequently formed ceramic layer after the ablation experiment. The FTIR peaks assigned to the vibrations of the methyl groups (—CH_3 deformation at 1413.9 cm^{-1}, —CH_3 wagging at 1261.44 cm^{-1}, —CH_3 stretching at 2963.28 cm^{-1}, C—H wagging at 1023.52 cm^{-1})[18] disappeared in the ceramic layer, which suggested the scission of Si—C in the silicone rubber side chains. The FTIR peak of Si—C (801.71 cm^{-1}) became weak, which could be ascribed to the destruction of the network formed by the interrelating of vinyl groups, resulting in the crack of the Si—C bond. However, the SiO volatile could react with the residual carbon which generated from matrix decomposition after ablation treatment, thus forming SiC. Moreover, the FTIR peak marked at 1599.65 cm^{-1} for the ceramic layer was attributed to the stretching vibration of C═C, suggesting the formation of residual carbon in the layer. The peak at 3428.76 cm^{-1} was assigned to the vibrations of end hydroxyl (O—H) which existed in partial/not terminated PMVS. When it comes to the ceramic layer, the peak became slightly stronger which was due to the formation of SiO_2 though condensation,[19] inducing the

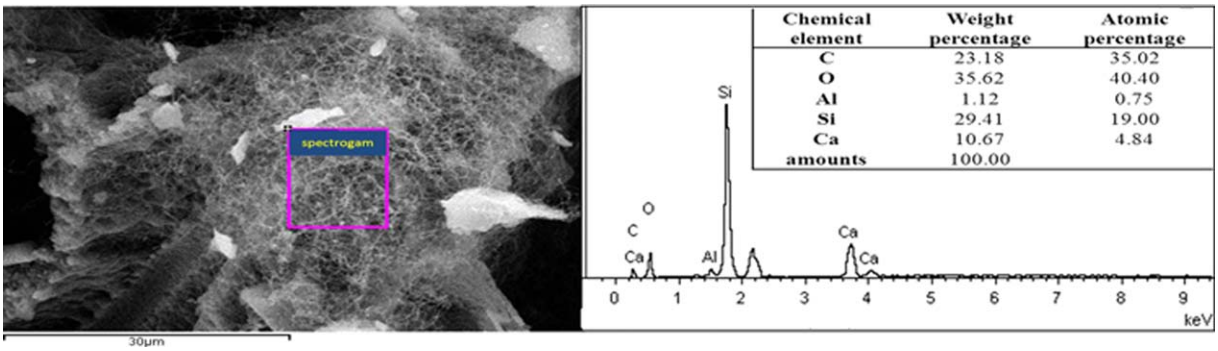

Figure 7. EDS of the filaments in the residual. [Color figure can be viewed in the online issue, which is available at wileyonlinelibrary.com.]

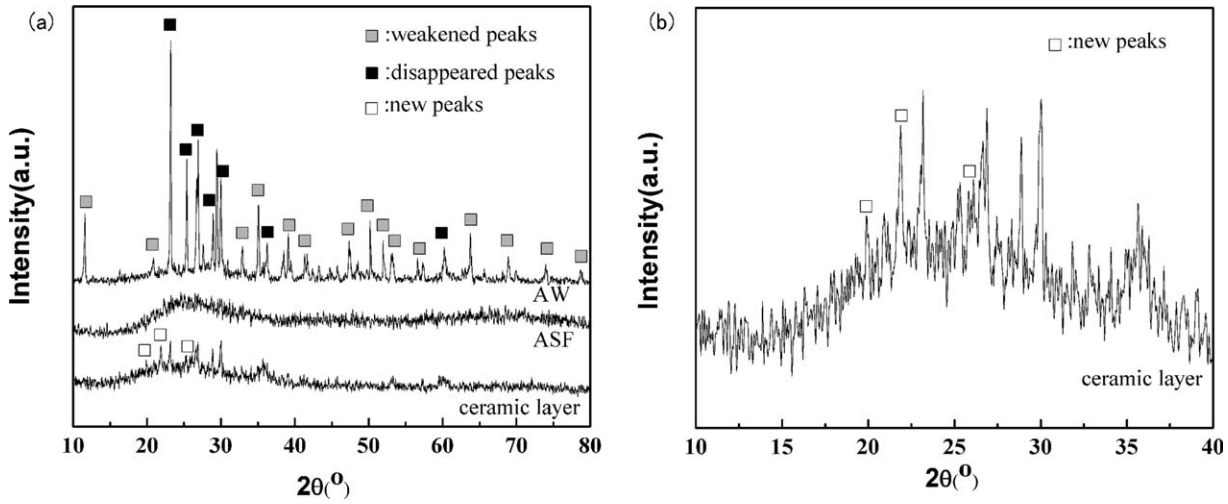

Figure 8. XRD patterns of the ceramic layer, ASF and AW.

development of hydroxyl (—OH). The peaks observed at 1094.04 and 470.47 cm^{-1} was respectively associated with the stretching and deformation vibration of Si—O bond, which existed in trimers, tetramers, SiO_2, AW, ASF, and matrix.

The energy dispersive spectrometer (EDS) study of the filaments is illustrated in Figure 7, which indicated the major components of the filaments were carbon, oxygen, and silicone. However, the minor component was attributed to the bottom base, which was mainly due to ASF and AW whose major constituents are $AlSiO_3$ and $CaSiO_3$, respectively. SiO volatile which was produced by the decomposition of rubber matrix, condensed on the surface of ceramic fiber and the residual after ablation treat, then formed SiO_2. While a portion of the volatile reacted with the residual carbon would form the SiC.[19–21] And the filaments improved the ablation resistance of the ablative composites by reducing the permeability of oxygen.

The XRD patterns for ASF, AW, and the ceramic layer are illustrated in Figure 8. The characteristic peaks observed at 22.31°, 12.21°, and 25.51° were attributed to SiO_2, silicone rubber and the residual carbon, respectively.[18] As shown in Figure 8, AW had many characteristic diffraction peaks.

Figure 8(b) shows that a weak broad convex was observed in the XRD patterns of the ceramic layer from 20° to 35°, which indicated that the amorphous ASF still existed in the layer. The

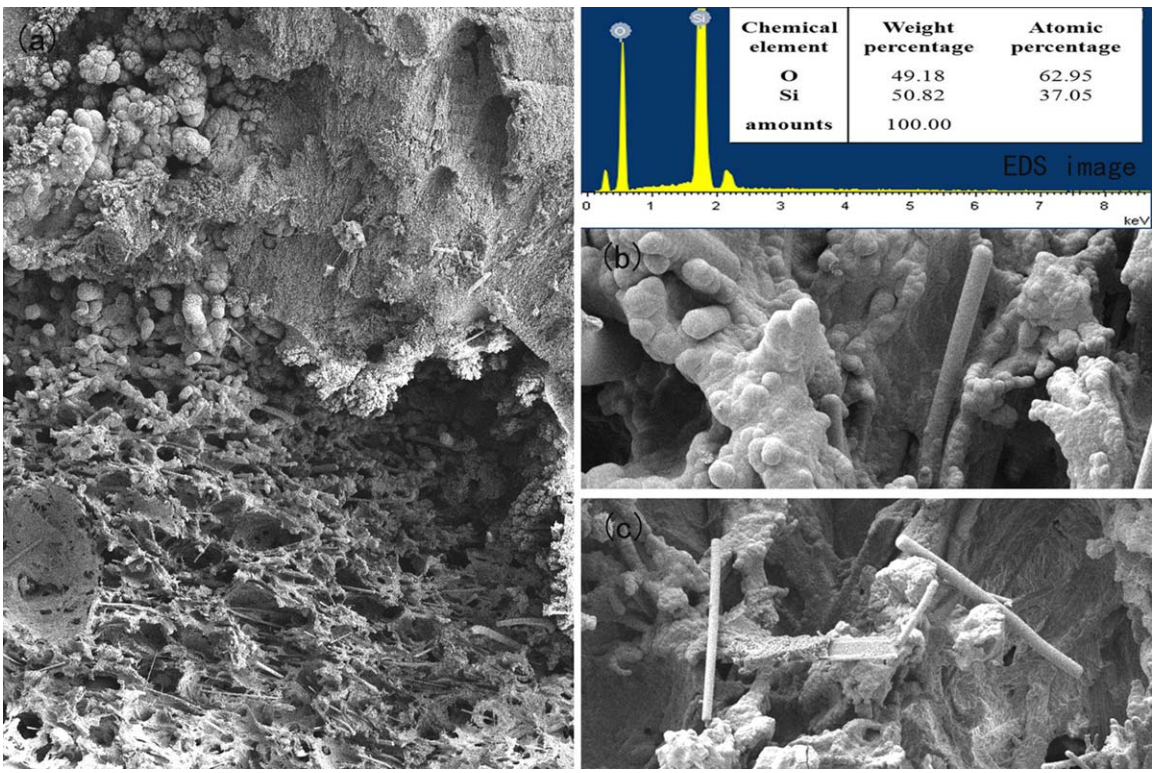

Figure 9. Transection SEM images of ceramic layer with the magnifications of (a) 50×, (b) and (c) 500×. [Color figure can be viewed in the online issue, which is available at wileyonlinelibrary.com.]

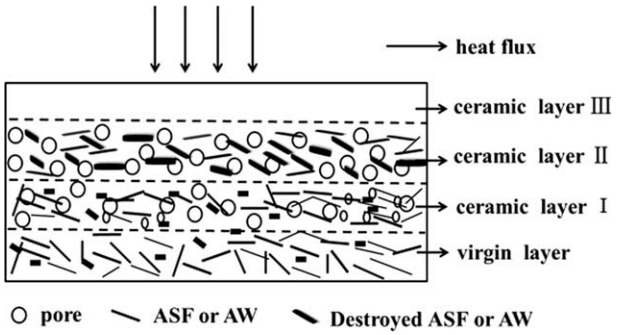

Figure 10. Schematic diagram of ablation mechanism.

new peaks were 19.2°, 21.67°, and 25.53°, which suggested the formation of SiO_2 and residual carbon. Notably, the characteristic peak of silicone rubber vanished from the ceramic layer, suggesting the decomposition of silicone rubber after ablation. However, the characteristic peaks of AW became weak, and some even disappeared, indicating that AW has taken part in reaction, and then turned into amorphous.

Ablation Mechanism

The high temperature heat flux generated from the oxyacetylene torch caused the degradation of the backbone of silicon rubber, while the rearrangement during the ablation process produced small siloxane molecules. Then a ceramic layer was observed after the ablation process was completed. ASF and AW with a certain length–diameter ratio could make the ceramic layer denser and harder, and thus reduce the line ablation rate of the composites.

After the oxyacetylene treatment, the silicon rubber in the composites decomposed by releasing small molecules gases and forming porous structure, as clearly shown in Figure 9(c) and Figure 10. However, the residual further decomposed during the ablation treatment, the ASF and AW were destroyed as is presented in Figures 9(b) and 10. With the reaction continuing, a white smooth layer was formed which was mainly due to the formation of amorphous SiO_2, acting as a protecting barrier in regions of low shear,[22] as shown in Figure 9 (the EDS image) and Figure 10. Theoretically, the ceramic layer was composed of three layers, as shown in Figure 10. The ceramic layer acted as a thermal shield with low thermal conductivity which could keep the heat from the oxyacetylene torch, and restrain combustible gas from exchanging with oxygen. The surface layer (ceramic layer **III**) was formed mainly through the melt of SiO_2 whose melting point is 1700°C, which reduced the permeability of oxygen and protected inner ceramic layer.

CONCLUSION

In this research, high ablation performance of silicon rubber composites was studied by oxyacetylene fire. TGA revealed that thermal stability of the ASF and AW modified silicone rubber improved compared with that of the neat rubber, which was mainly ascribed to the low thermally conducting surface layer formed during the heat treatment, hindering the heat flux from penetrating into the internal matrix. Moreover, the addition of ASF and AW was beneficial to the evaluation of the ablation properties of the composites by forming a dense ceramic layer during the fire treatment. The SiO volatile produced during fire treatment would condense or react with the residual carbon, forming SiO_2/SiC filaments, which could reduce the permeability of oxygen. The densest ceramic layer and the optimum ablation properties were observed at the proportion of 20/40 phr (ASF/AW) in the rubber composites.

ACKNOWLEDGMENTS

The authors would like to thank National Natural Science Foundation of China (51273118) and the Science and Technology Pillar Program of Sichuan (2013FZ0006) for financial support, and the Analytical and Testing Center of Sichuan University for providing SEM measurement.

REFERENCES

1. Natali, M.; Monti, M.; Puglia, D.; Kenny, J. M.; Torre, L. *Compos. A* **2012**, *43*, 174.
2. Gao, G. X.; Zhang, Z. C.; Li, X. F.; Meng, Q. J.; Zheng, Y. S. *Polym. Bull.* **2010**, *64*, 607.
3. Paydayesh, A.; Kokabi, M.; Bahramian, A. R. *J. Appl. Polym. Sci.* **2012**, DOI:10.1002/app.37588.
4. Vaia, R. A.; Price, G.; Ruth, P. N.; Nguyen, H. T.; Lichtenhan. *Appl. Clay Sci.* **1999**, *15*, 67.
5. Bahramian, A. R.; Kokabi, M. *J. Hazard. Mater.* **2009**, *166*, 445.
6. Yang, D.; Zhang, W.; Jiang, B. Z.; Guo, Y. *Compos. A Appl. S.* **2013**, *44*, 70.
7. Hanu, L. G.; Simon, G. P.; Cheng, Y.-B. *Polym. Degrad. Stabil.* **2006**, *91*, 1373.
8. Kim, E. S.; Lee, T. H.; Shin, S. H.; Yoon, J.-S. *J. Appl. Polym. Sci.* **2011**, *120*, 831.
9. Kim, E. S.; Kim, E. J.; Shim, J. H.; Yoon, J.-S. *J. Appl. Polym. Sci.* **2008**, *110*, 1263.
10. Chen, Z. F.; Fang, D.; Miao, Y. L.; Yan, B. *Corros. Sci.* **2008**, *50*, 3378.
11. Gallego, N. C.; Edie, D. D. *Compos. A Appl. S.* **2001**, *32*, 1038.
12. Nayar, P.; Khanna, A. *Vacuum* **2013**, *89*, 17.
13. Mansouri, J.; Burford, R. P.; Cheng, Y. B.; Hanu, L. *J. Mater. Sci.* **2005**, *40*, 5741.
14. Mansouri, J.; Burford, R. P.; Cheng, Y. B. *Mater. Sci. Eng. A* **2006**, *425*, 7.
15. Sun, Z. M.; Bai, Z. Q.; Shen, H. L.; Zheng, S. L.; Ray, L. F. *Mater. Res. Bull.* **2013**, *48*, 1013.
16. Gordon, S. H.; Mohamed, A.; Harry-o'kuru, R. E.; Imam, S. H. *Appl. Spectr.* **2010**, *64*, 448.
17. Oyumi, Y. *J. Polym. Sci. A Polym. Chem.* **1998**, *36*, 233.
18. Yang, D.; Zhang, W.; Jiang, B. Z. *Ceram. Int.* **2012**, *39*, 1575.
19. Gumula, T.; Blazewicz, S. *Ceram. Int.* **2013**, *39*, 3795.
20. Ryu, Z. Y.; Zheng, J. T.; Wang, M. Z.; Zhang, B. *J. Carbon* **2001**, *39*, 1929.
21. Gumula, T.; Michalowski, J.; Blazewicz, M.; Blazewicz, S. *Ceram. Int.* **2010**, *30*, 749.
22. Sandén, R. *Polym. Test.* **2002**, *21*, 61.